Crystallization Behavior of Poly(*N*-methyldodecano-12-lactam). III. Kinetics of Isothermal Crystallization

J. Kratochvíl, A. Sikora

Institute of Macromolecular Chemistry, Academy of Sciences of the Czech Republic, Heyrovského nám. 2, 162 06 Prague 6, Czech Republic

Received 18 June 2003; accepted 15 February 2004
DOI 10.1002/app.20444
Published online in Wiley InterScience (www.interscience.wiley.com).

ABSTRACT: Differential scanning calorimetry, combined with Avrami theory, was used to investigate the kinetics of three steps of the complex crystallization process of poly(*N*-methyldodecano-12-lactam) (MPA): (1) primary melt crystallization at respective crystallization temperature (T_c), (2) additional crystallization at 30°C, and (3) recrystallization at 54°C. Kinetics of the three steps was discussed with respect to T_c. The Avrami exponent n of primary melt crystallization decreased between 2.5 and 1.9 in the range of T_c values of −10 to 20°C, which suggests heterogeneous nucleation, followed by two-dimensional growth, with a larger involvement of homogeneous thermal nucleation at greater supercoolings. The crystallization rate constant k decreased with increasing T_c. The value of $n = 1.5$ for additional crystallization implies a two-dimensional diffusion-controlled crystal growth with a suppressed nucleation phase. For T_c values ranging from −10 to 0°C and 0 to 20°C, k showed weak and quite strong decreasing dependencies on T_c, respectively. The recrystallization mechanism involved partial melting of primary crystallites and two-dimensional rearrangement of chains into a more perfect structure. The rate of this process was almost independent of T_c. The values of activation energies were derived for the three steps of MPA crystallization using the Arrhenius equation. © 2004 Wiley Periodicals, Inc. J Appl Polym Sci 93: 279–293, 2004

Key words: poly(*N*-methyldodecano-12-lactam) (MPA); crystallization; kinetics (polym.); Avrami theory; differential scanning calorimetry (DSC)

INTRODUCTION

In the first two parts of this series[1,2] we studied the crystallization/melting behavior of poly(*N*-methyldodecano-12-lactam) (MPA) and suggested a molecular interpretation of the observed phenomena. DSC, X-ray, and spectroscopic measurements revealed a complex crystallization/melting behavior of MPA. The processes taking place during isothermal melt crystallization and subsequent DSC run can be described as three consecutive steps, as follows:

1. After cooling from the melt to the crystallization temperature (T_c values of −23 to 7°C), a primary lamellar structure is formed, which melts at about 51°C. During later stages of isothermal crystallization, imperfect "fringed" crystallites melting at about T_c + 10°C are formed in the interlamellar space of the primary structure.
2. On heating, additional crystallization of the primary lamellae melting at 51°C occurs. The optimum temperature of this additional crystallization is about 30°C. In the case of isothermal crystallization from the melt at T_c values of 17 to 32°C, the two stages of the primary structure formation apparently combine into a single isothermal step.
3. On further heating, the primary crystallites undergo recrystallization, with formation of a final higher-ordered structure that melts at about 62°C. The optimum temperature of recrystallization is about 54°C.

Crystallization/recrystallization of MPA is a kinetic process dependent on molecular weight and the rate of temperature changes. On the molecular level, the crystallization/recrystallization processes taking place in MPA can be interpreted as being directed by two conformational transitions in MPA molecules, that is, the *trans–cis* transition on the C—N bond and the *gauche–trans* transition of the C—C sequences.

In the present study we have attempted to evaluate the three above-mentioned crystallization steps with respect to kinetics. A generally accepted instrument in studying the crystallization kinetics of polymers is the Avrami theory.[3,4] The following Avrami equation relates the relative crystallinity $X(t)$ of a polymer to crystallization time t:

$$X(t) = 1 - \exp(-kt^n) \quad (1)$$

Correspondence to: J. Kratochvíl (jakr@imc.cas.cz).
Contract grant sponsor: Grant Agency of the Academy of Sciences of the Czech Republic; contract grant number: A4050007.

The evaluation of data measured at given T_c provides two kinetic parameters. The Avrami exponent n is related to the nucleation mechanism and dimensionality of crystal growth; the kinetic constant k is a function of nucleation density and rate of crystal growth.

Adoption of the Avrami equation for polymer systems is based on several assumptions and simplifications. The most important of them are as follows[5–7]:

- Constant density and rate of nucleation
- Random distribution of nuclei in the melt
- Uniqueness of the nucleation mode, either heterogeneous or homogeneous
- A jump in change of the crystallization rate from zero to a constant value after reaching a critical dimension of nuclei
- Constant radial rate of crystal growth in an infinite volume
- No change in polymer density during crystallization
- Only initial stages of crystallization are involved, with no secondary crystallization and impingement of growing crystallites

Under these assumptions, the Avrami exponent n should have an integer value of 1, 2, or 3 for one-, two-, or three-dimensional crystal growth geometry, respectively, with heterogeneous athermal nucleation. In the case of homogeneous thermal nucleation the value of n should be higher by 1.

Not all the above-mentioned assumptions are usually met in polymer systems. Consequently, deviations from theoretical expectations are often found. The most frequent of them are as follows:

- Broken or curved character of the double-logarithmic Avrami plots
- Noninteger value of the Avrami exponent
- Dependency of the Avrami exponent on crystallization temperature
- Values of $n > 4$

Various, in some cases contradictory, interpretations of these deviations can be found in the literature. Nonlinearity of the Avrami plots is usually accounted for by secondary crystallization, onset of impingement of growing crystallites, and/or change in crystal perfection.[8,9]

Fractional values of the Avrami exponent are quite often encountered in polymer systems. They are generally associated with noncompliance with some of the assumptions adopted in deriving the Avrami equation.[6] Interpretations of these noninteger n values include mixed nucleating and/or growth modes,[10] variability of growth dimensionality,[11] involvement of secondary crystallization,[10–12] change in rate of nucleation and/or crystal growth during crystallization,[13] and change in the ratio of densities of crystalline and amorphous materials.[14] A relatively often ascertained n value of about 2.5 is explained by simultaneous occurrence of two- and three-dimensional crystal growth, including formation of a sheaflike structure during early stages of crystallization.[13–15]

The Avrami exponent was also found to be temperature dependent. The increase in n values with decreasing crystallization temperature is explained by greater involvement of homogeneous nucleation at higher supercoolings[15,16] or by multidimensional growth.[17] On the other hand, the increase in n with rising crystallization temperature is interpreted as a combination of one-dimensional growth with two-dimensional thermal-nucleated crystal growth.[18,19] The transition from the diffusion- to nucleation-controlled crystallization mode was found to be associated with an increase in the n value from 1.5 to 3.0.[20] The values of Avrami exponents > 4 were attributed to curing of crystallizing thermosets[10] or to shear forces.[20]

In this study we attempted to apply the Avrami theory to investigate the kinetics of the three isothermal steps involved in the complex crystallization process of MPA:

1. Crystallization from the melt at a given crystallization temperature (T_c values of -10 to 20°C)
2. Additional crystallization at its optimum temperature (30°C)
3. Recrystallization at its optimum temperature (54°C)

Each of the later steps (2 and 3) was investigated after completion of the previous step and their kinetics are discussed with respect to the original T_c.

EXPERIMENTAL

The samples of MPA used in this study were the same as those in the previous parts. The samples denoted MPA 5, MPA 15, and MPA 45 have weight-average molecular weights of 5000, 15,000, and 45,000, respectively. A Perkin–Elmer Pyris 1 DSC apparatus (Perkin Elmer Cetus Instruments, Norwalk, CT) was used for the calorimetric measurements. The weight of samples closed in aluminum pans was about 10 mg. For details on the samples and basic instrumentation, the reader is referred to the previous articles.[1,2]

Individual crystallization exotherms were scanned under specified isothermal conditions for the three crystallization steps: melt crystallization, additional crystallization, and recrystallization. A multistep program was used in the DSC measurements, which made it possible to successively record the exotherms for all three crystallization steps corresponding to the given initial crystallization temperature T_c.

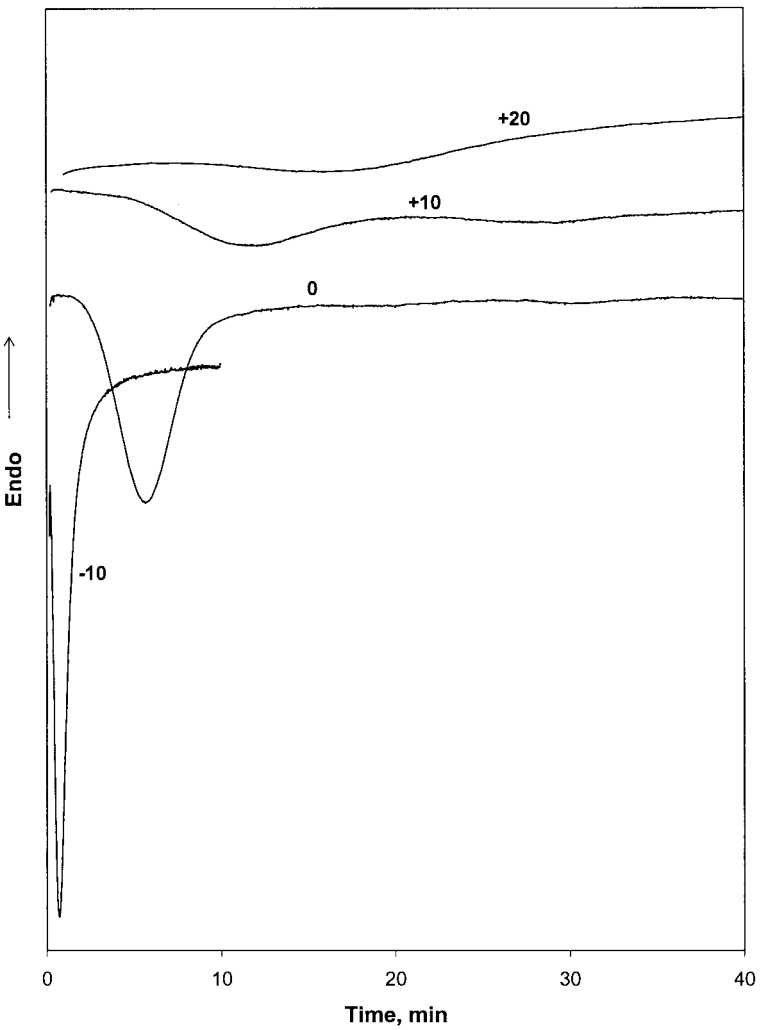

Figure 1 Exotherms of primary melt crystallization of MPA 5 at indicated T_c (°C).

After inserting the sample pan into the DSC apparatus, the temperature was rapidly increased to 90°C and kept there for 10 min to remove all traces of crystallinity. Then, the sample was rapidly cooled to the given T_c in the range of −10 to 20°C and kept at this temperature for a certain period of time necessary for complete development of the melt crystallization exotherm. In the subsequent step, the temperature was rapidly increased to 30°C and kept there for a certain period of time necessary for complete recording of the additional crystallization exotherm. Thereafter, the temperature was rapidly increased to 54°C and kept there for a necessary period, during which the recrystallization exotherm was recorded. The rate of all temperature jumps was ±200°C/min.

RESULTS AND DISCUSSION

Primary crystallization from the melt

The exotherms of MPA recorded during the first isothermal crystallization step (melt crystallization) are shown in Figure 1. The time necessary for completion of the primary exotherm ranged between 3.0 min (MPA 5, −10°C) and 145 min (MPA 45, 20°C). The marked difference in shape of the respective exotherms provides evidence of a strong dependency of the primary crystallization process on T_c.

The corresponding experimental cumulative crystallization isotherms of MPA 5 are shown as solid lines in Figure 2. The curves are of a typical sigmoid character. The induction time representing the onset of melt crystallization was found to increase dramatically with T_c, reaching the value of about 6 min for the MPA 5 crystallization at 20°C.

Initial parts of the double-logarithmic Avrami plots of melt crystallization of MPA samples at the respective T_c (Fig. 3) provide the kinetic parameters: the Avrami exponent n and kinetic constant k. These results are summarized in Figure 4(a) and (b), where the kinetic parameters of melt crystallization are plotted against crystallization temperature.

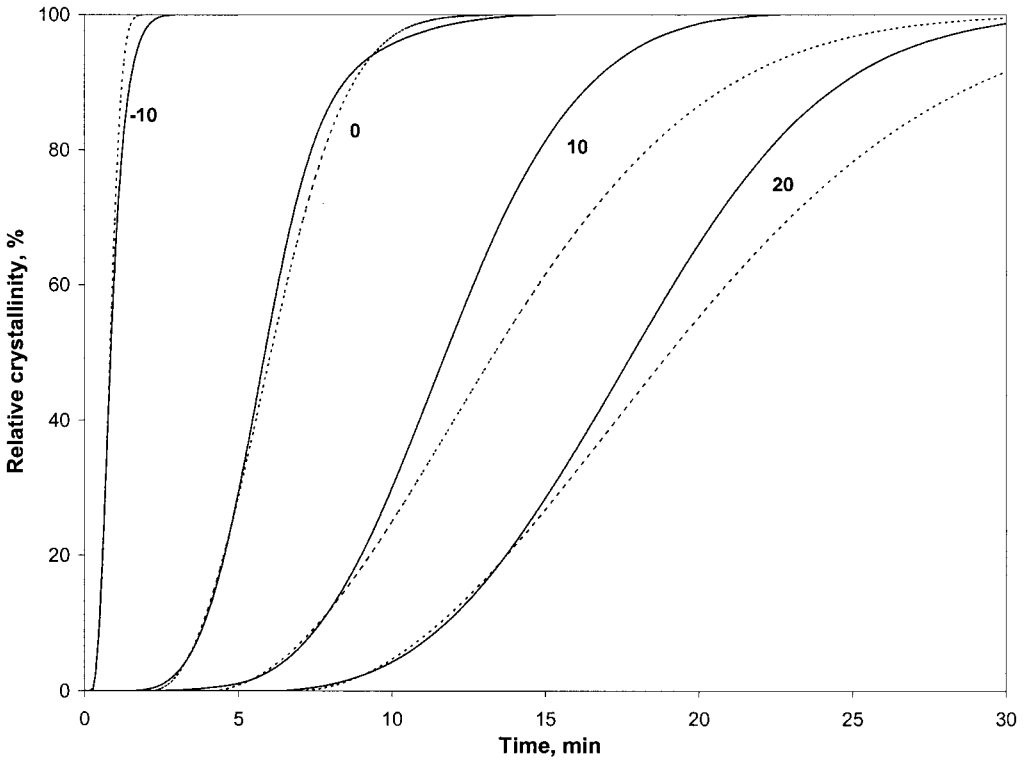

Figure 2 Crystallization isotherms of primary melt crystallization of MPA 5 at indicated T_c (°C): solid lines, experimental; dotted lines, calculated.

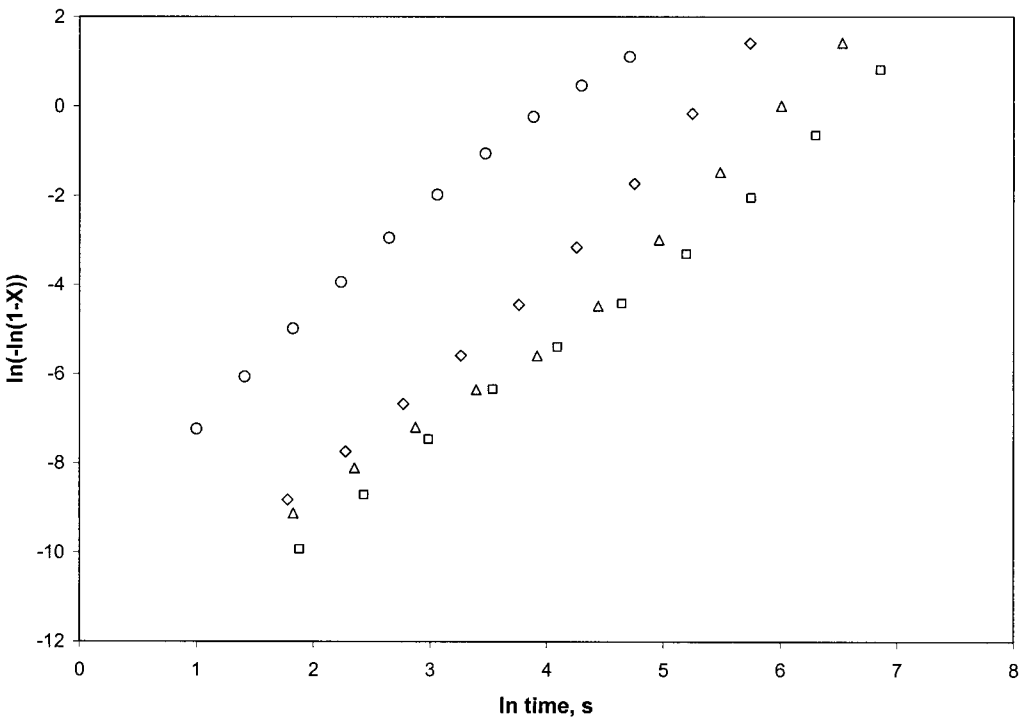

Figure 3 Avrami plots of primary melt crystallization of MPA 5 at respective T_c: ○ −10°C; ◇ 0°C; △ 10°C; □ 20°C.

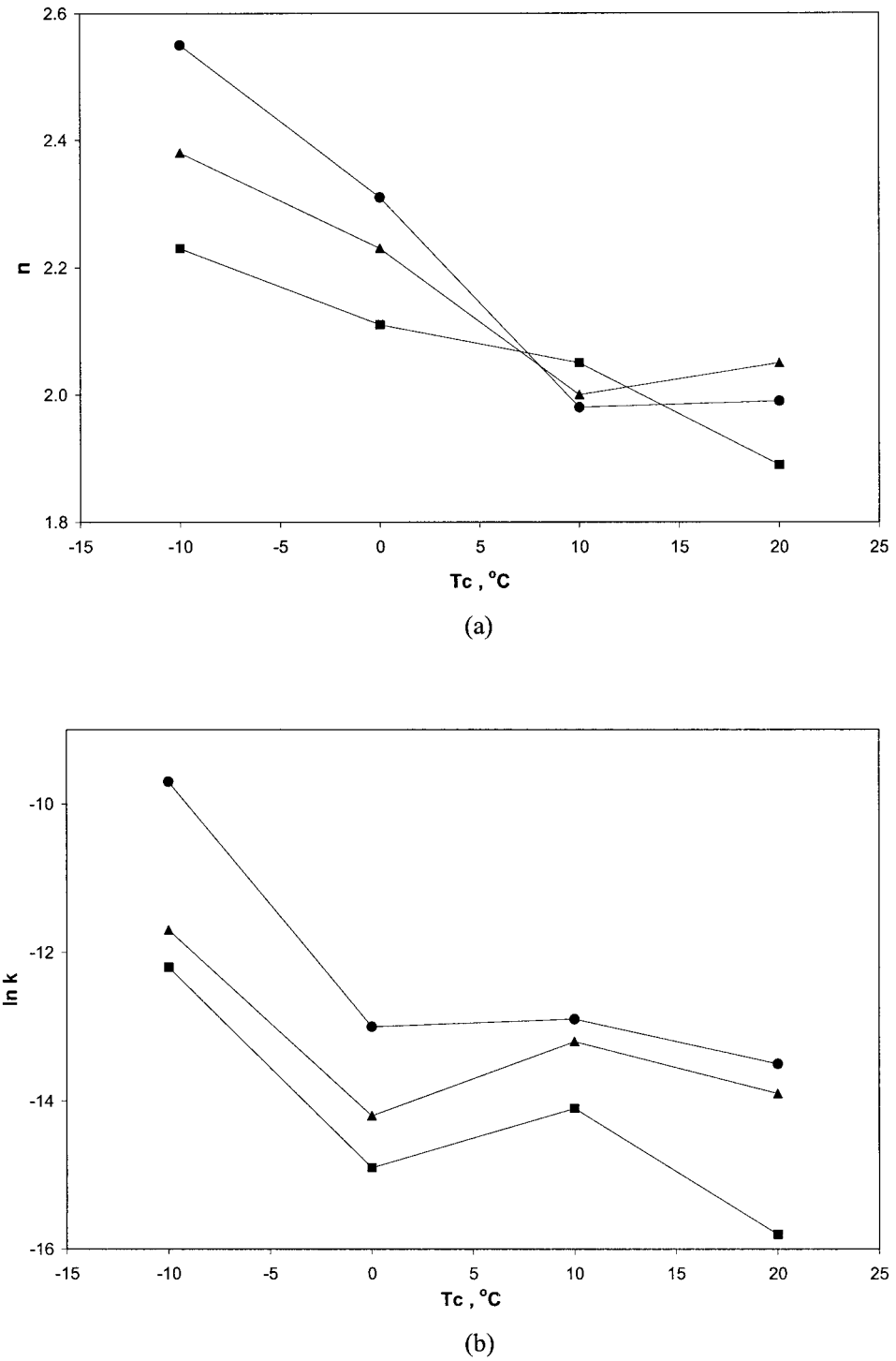

Figure 4 Dependency of kinetic parameters of primary melt crystallization on crystallization temperature T_c: (a) Avrami exponent, (b) logarithm of rate constant; ● MPA 5; ▲ MPA 15; ■ MPA 45.

The values of the Avrami exponent n range between 2.5 and 1.9 and their decreasing trend with rising T_c is apparent from Figure 4(a). These observed values of the Avrami exponent suggest heterogeneous athermal nucleation followed by two-dimensional lamellar crystal growth. At greater supercoolings, the homogeneous thermal nucleation is apparently involved to a greater extent.

The kinetic constant k, evaluated from the initial parts of the Avrami plots, shows a general decreasing trend with increasing crystallization temperature, which is typical of nucleation-controlled crystallization mode.[6,21] However, the dependencies in Figure 4(b) are not monotonic and a local maximum of crystallization rate is apparent for the crystallization temperature at about 10°C. This temperature lies almost in

the middle of the crystallization window between glass-transition temperature ($T_g \sim -40$°C) and melting temperature ($T_m \sim 60$°C) of MPA. However, unlike many other polymers showing maximum of crystallization rate at temperatures around the middle of the crystallization window and then decreasing trend as temperature approaches T_g,[21] the crystallization rate of MPA, after passing a local minimum at 0°C, increases with decreasing temperature. In our previous study[1] we found that at −23°C crystallization of MPA was so fast that its kinetics could not be measured. Our recent study of nonisothermal crystallization of MPA[22] has shown that, after cooling to below T_g, the subsequent heating runs show crystallization exotherms starting as low as at about T_g + 5°C. The explanation, of course quite tentative, of this rather peculiar behavior of MPA could be seen in combination of the relatively high mobility of MPA chains, facilitated by their molecular structure and two conformational transitions,[1,2] and a strong involvement of thermodynamic fluctuations, leading to homogeneous nucleation at temperatures close to T_g. The authors are not familiar with a reference to similar behavior of a polymer in the literature.

The determined parameters n and k were used for calculating cumulative crystallization isotherms. Coincidence of experimental and calculated cumulative curves can then be used as a criterion of validity of the Avrami approach. This comparison is shown in Figure 2. One can see that at $T_c = -10$°C the Avrami approach is valid up to a relative crystallinity of about 60%, and at 0°C, to about 30%. At 10 and 20°C a relatively good agreement of the curves was found for the crystallinities up to about 10–15% only. This fact is in agreement with the general concept of the Avrami theory being applicable to initial phases of crystallization only.[3,4,21]

Additional crystallization

Before discussing the results of the additional crystallization kinetics of MPA, we consider it reasonable to briefly sum up which processes, to our knowledge,[1,2] proceed in the system during the first two stages of the complex crystallization of MPA, melt and additional crystallization.

After cooling the polymer melt to the given crystallization temperature T_c, an equilibrium is established between the *cis* and *trans* C—N conformers and melt crystallization takes place, in which chain sequences with predominant *cis* C—N conformations are involved. During this process the primary lamellar structure is formed with the maximum of melting endotherm ($T_m \approx 51$°C). At later stages of melt crystallization, the secondary "fringed" micelles with T_m equal to about T_c + 10°C are formed in the interlamellar amorphous phase. On heating, either during the DSC scan or on a sharp temperature jump, this secondary structure partially melts. The *trans–cis* equilibrium shifts toward the *cis* form and, at about 30°C, a cooperative *trans–cis* transition takes place in the system, which facilitates additional crystallization associated with a sharp exotherm. During this additional crystallization step, the same structure ($T_m \approx 51$°C) is formed as that during the primary melt crystallization at the given T_c.

In the present study, all the additional crystallization runs were carried out at the same temperature of 30°C, which corresponds to the mean value of peak temperature of the additional crystallization exotherms on the DSC runs.[1] However, the whole discussion of temperature dependencies of kinetic parameters of additional crystallization is related to the particular *primary* (melt) crystallization temperatures T_c. Thus, the results presented in this article reflect the effect that the conditions of melt crystallization at the given T_c have on the course of additional crystallization.

The exotherms of MPA 5 scanned at 30°C after melt crystallization at the given T_c are shown in Figure 5. The time necessary for completion of the additional crystallization exotherm ranged between 2.6 min (MPA 5, $T_c = -10$°C) and 66 min (MPA 45, $T_c = 20$°C). The main difference in the character of these exotherms, compared with those of melt crystallization (Fig. 1), is their sharp onset, making exact specification of the beginning of exotherm t_0 somewhat disputable. We have adopted the procedure applied by several authors in which t_0 is identified as a point of intersection of the initial exotherm branch with the extended asymptote at long times.[23]

In the first of this series of studies[1] on isothermal crystallization we concluded that at higher T_c the two steps, melt and additional crystallization, seem to be combined into a single step, given that no exotherm at about 30°C was detected in the DSC heating runs after isothermal crystallization at $T_c \geq 17$°C. However, this apparent absence of the additional crystallization exotherm was obviously a consequence of mutual compensation of heat flows associated with parallel/consecutive processes occurring during the DSC scan (i.e., additional crystallization plus melting of the primary crystalline structure). In fact, the additional crystallization exotherm, as scanned in the present study at 30°C after primary isothermal melt crystallization at 20°C, was quite well developed and could be evaluated.

The experimental cumulative additional crystallization isotherms of MPA 5 are shown as solid lines in Figure 6. The curves feature a relatively sharp onset, which implies that additional crystallization reaches its maximum rate quite soon after the system temperature is increased to 30°C. The isotherms, especially those after low T_c, include almost no run-in period

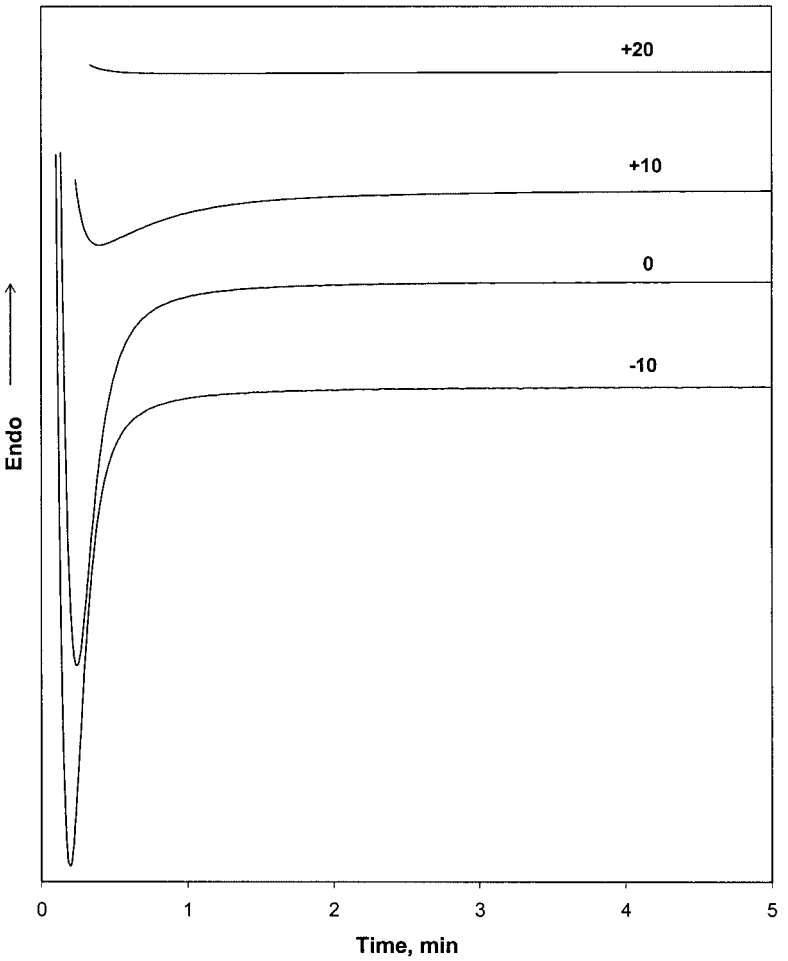

Figure 5 Exotherms of additional crystallization of MPA 5 at 30°C after melt crystallization at indicated T_c (°C).

characteristic of the primary melt crystallization (Fig. 2). It is also apparent from Figure 6 that, for T_c values ranging from −10 to 0°C, the course of additional crystallization is virtually independent of the melt crystallization temperature. On the other hand, at higher T_c the effect of temperature is quite strong.

Figure 7 shows double-logarithmic Avrami plots obtained by stepwise integration of the exotherms in Figure 5. The kinetic parameters evaluated from the initial linear parts of the Avrami plots of additional crystallization are shown in Figure 8(a) and (b).

The values of Avrami exponent n fall within a narrow range around 1.5 and are virtually independent of the original melt crystallization temperature. The value of $n = 1.5$ is often associated with the diffusion-controlled crystallization mode.[18,20] Tan et al.[24] studied the kinetics of crystallization from the metastable melt obtained by partial melting of imperfect structures formed during secondary crystallization. The authors obtained the values of $n = 1.0$ to 1.2. They also concluded that no nucleation process was involved in the kinetics and crystallites grew from the metastable melt directly on the surface of the primary structure.

From the shape of the additional crystallization exotherms in Figure 5 and the cumulative isotherms in Figure 6, we can suggest that the kinetic nucleation phase is apparently absent. This would explain the value of $n = 1.5$ for the two-dimensional diffusion-controlled crystal growth mode. This dimensionality can logically be expected as a continuation of the two-dimensional nucleation-controlled mechanism of the primary crystallization of MPA from the melt discussed above. In fact, as we found in our previous study,[1] no change in T_m, and hence in lamellar thickness, occurs during additional crystallization and just the amount of the primary lamellae ($T_m \approx 51$°C) increases during the additional crystallization stage.

The values of the kinetic constant k [Fig. 8(b)] show that, regarding the effect of the primary crystallization temperature, the results of additional crystallization kinetics can be divided into two ranges. In the range of T_c values of −10 to 0°C, the kinetic constant k is almost independent of temperature of the first crystallization step. In the range of T_c values of 0 to 20°C, it sharply decreases with increasing T_c. Apparently, the primary crystallites formed at these temperatures during the

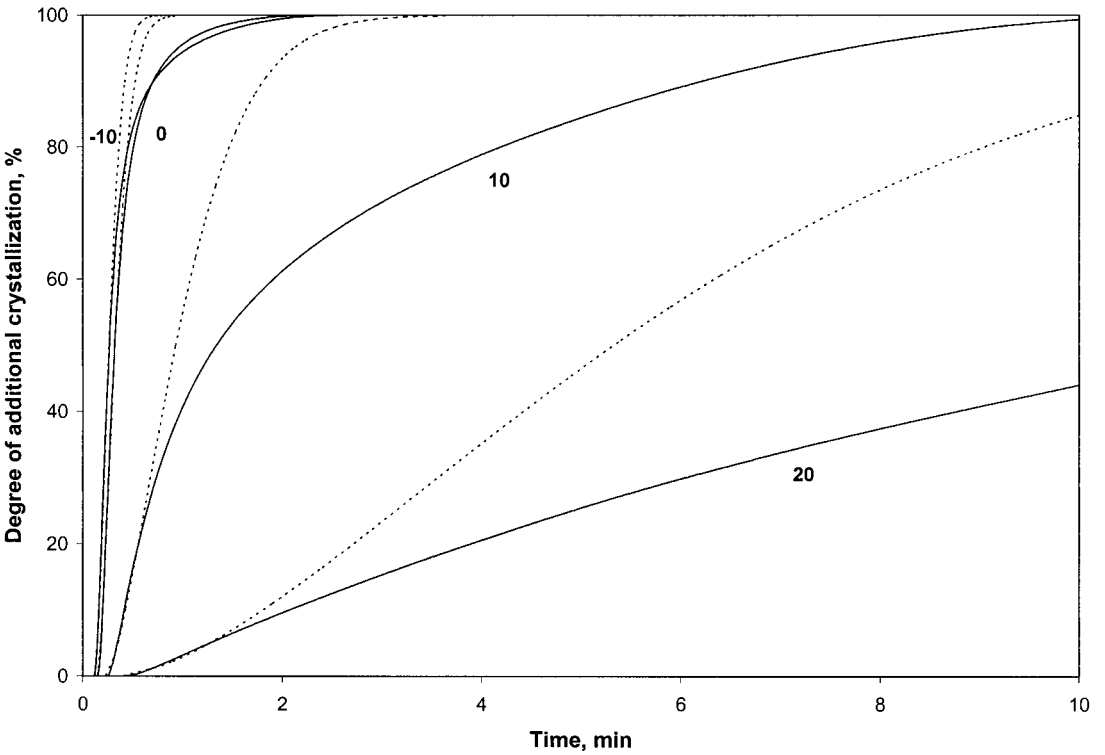

Figure 6 Crystallization isotherms of additional crystallization of MPA 5 at 30°C after melt crystallization at indicated T_c (°C): solid lines, experimental; dotted lines, calculated.

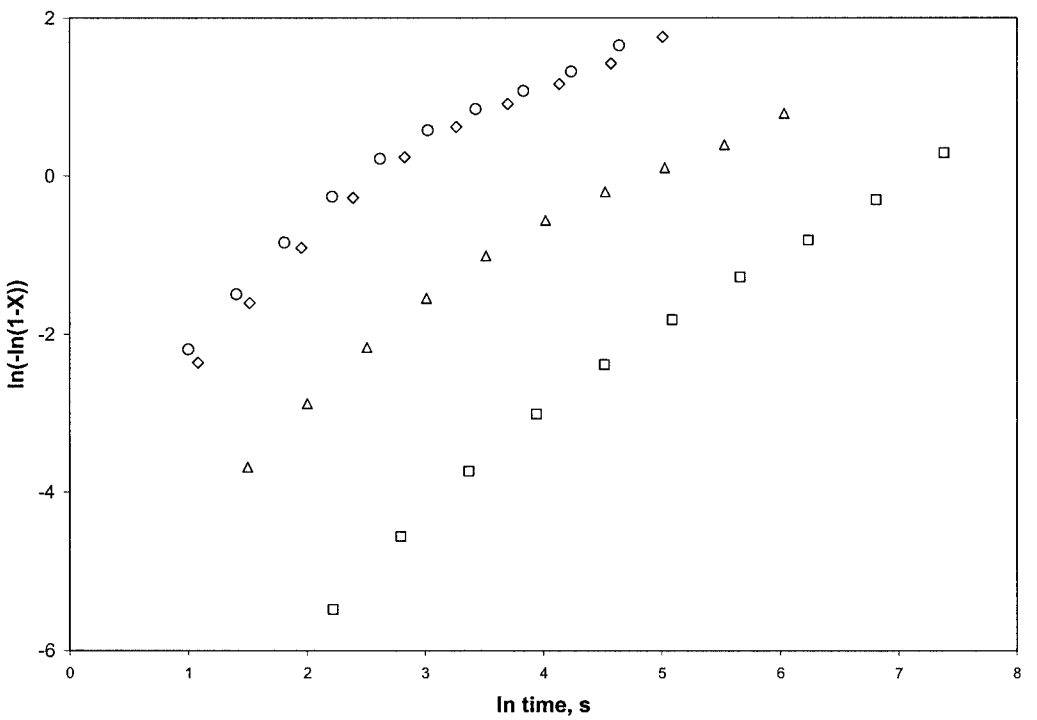

Figure 7 Avrami plots of additional crystallization of MPA 5 at 30°C after melt crystallization at respective T_c: ○ −10°C; ◇ 0°C; △ 10°C; □ 20°C.

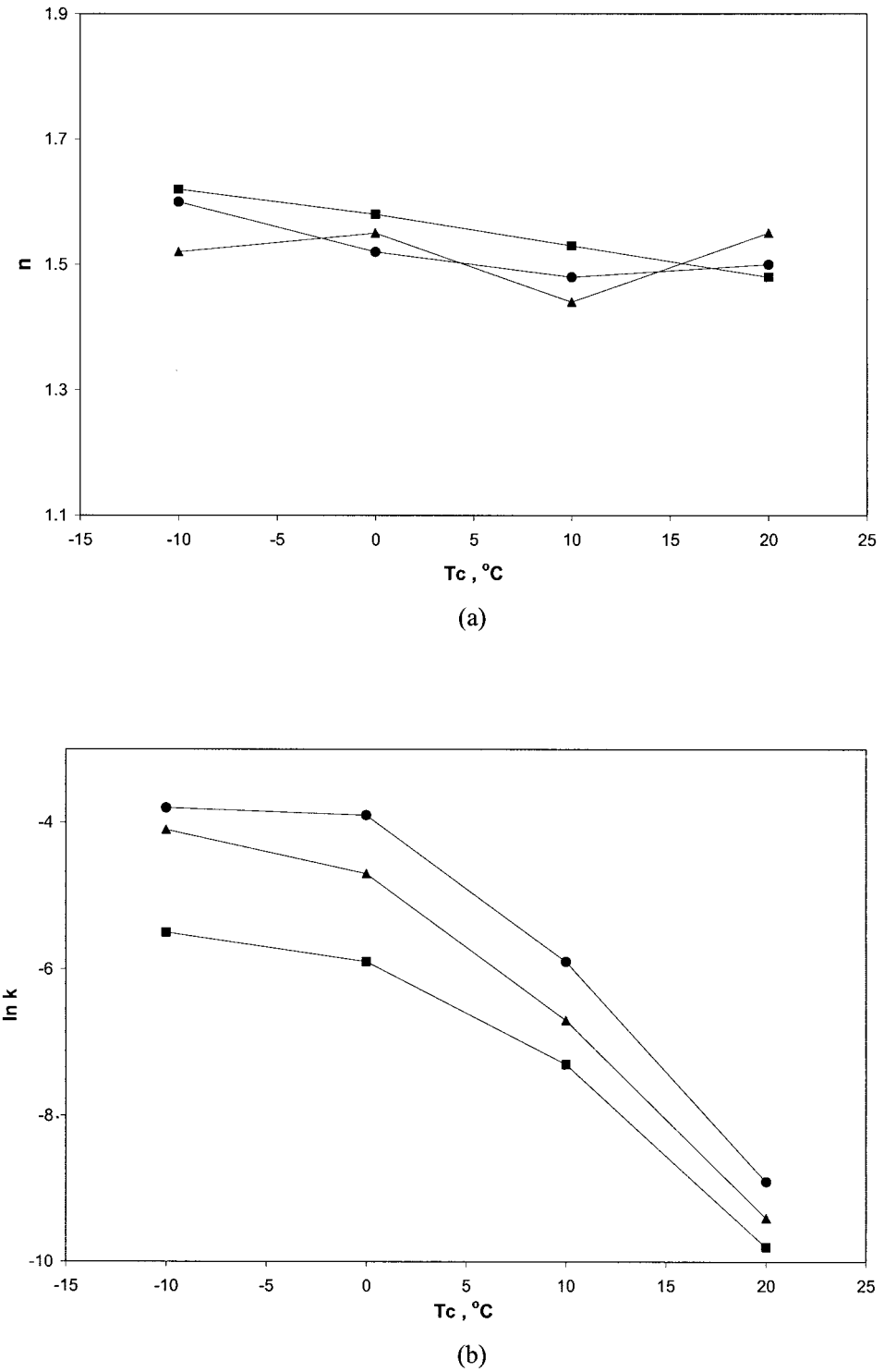

Figure 8 Dependency of kinetic parameters of additional crystallization on melt crystallization temperature T_c: (a) Avrami exponent, (b) logarithm of rate constant; ● MPA 5; ▲ MPA 15; ■ MPA 45.

melt crystallization do not provide enough sites for additional crystal growth, which results in slowing down of the additional crystallization process. However, as made clear from comparison of the kinetic constants k in Figures 4(b) and 8(b), additional crystallization is by several orders of magnitude faster than primary crystallization from the melt. This reflects the fact that the nucleation phase is virtually absent in the additional crystallization process of MPA and crystallites grow directly on the primary lamellar structure, the process being facilitated by the cooperative *trans–cis* transition on the C—N bond at 30°C.

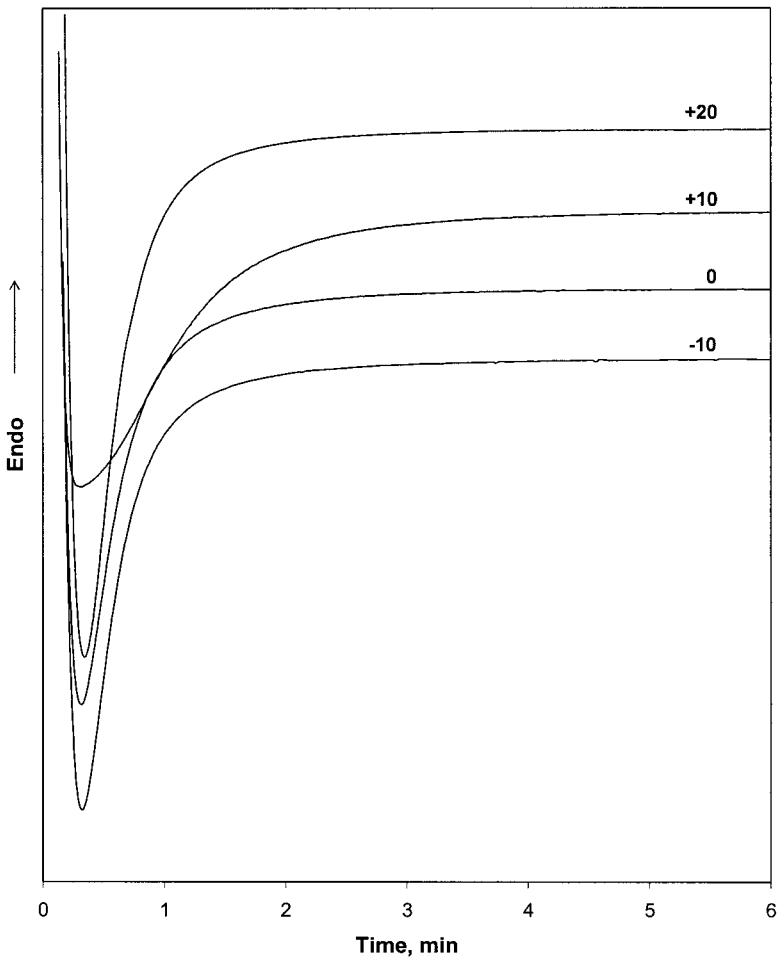

Figure 9 Exotherms of recrystallization of MPA 5 at 54°C after melt crystallization at indicated T_c (°C) and additional crystallization at 30°C.

Similarly to the discussion reported in the previous article on primary crystallization kinetics, comparison of experimental and calculated cumulative curves is presented in Figure 6. One can see that, in additional crystallization of MPA, the Avrami approach is valid up to relative crystallinities of about 60% for T_c values of −10 and 0°C. Its validity is, however, limited to about 20 and 10% for T_c values of 10 and 20°C, respectively.

Recrystallization

In view of our previous study,[2] the crystalline structure of MPA formed during the first two stages—melt crystallization at respective T_c and additional crystallization at 30°C—shows a relatively high degree of perfection but, still, the hydrocarbon sequences of MPA chains in this structure include irregularities associated with the *gauche* C—C conformations. On heating, either during the DSC run or on a temperature jump, the primary crystalline structure ($T_m \approx$ 51°C) partially melts; the number of *gauche* defects decreases until, at about 54°C, a cooperative transition takes place during which the all-*trans* CH_2 sequences are arranged in MPA chains; and the system recrystallizes to the final, more perfect crystalline structure with the melting temperature about 62°C. Recrystallization of MPA is associated with an increase in the long period of about 12% and approximately the same increase in crystallinity.

The recrystallization exotherms of MPA were scanned at 54°C in the third step of a particular DSC run, following the melt crystallization at respective T_c and additional crystallization at 30°C. Hence, all results of recrystallization kinetics are discussed with respect to the effect that the preceding two steps have on the course of final recrystallization.

The recrystallization exotherms of MPA are shown in Figure 9. The time necessary for their completion ranged between 5.5 min (MPA 5, $T_c = -10$°C) and 8.3 min (MPA 45, $T_c = 20$°C). Because the shape of the recrystallization exotherms is similar to that of the

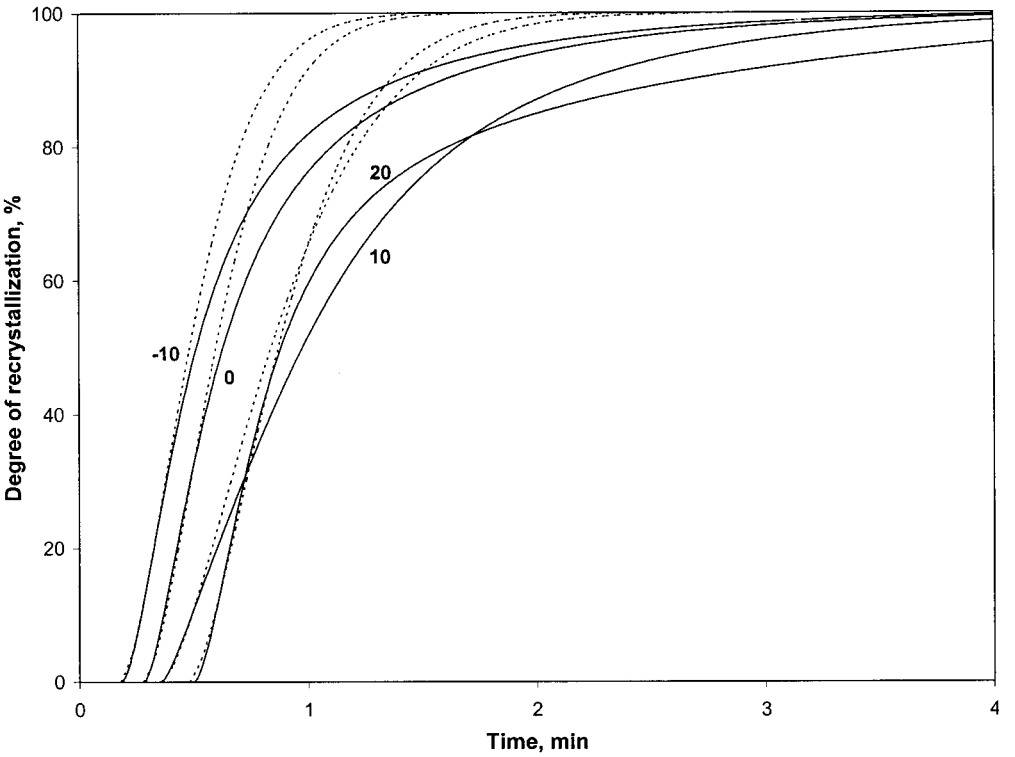

Figure 10 Isotherms of recrystallization of MPA 5 at 54°C after melt crystallization at indicated T_c (°C) and additional crystallization at 30°C; isotherms for T_c = 0, 10, and 20°C are shifted along the *x*-axis; solid lines, experimental; dotted lines, calculated.

exotherms of additional crystallization (Fig. 5), the same procedure was adopted in setting the starting time t_0 of the exotherms.

The experimental cumulative recrystallization isotherms are shown as solid lines in Figure 10. (The isotherms for T_c values of 0, 10, and 20°C have been shifted along the *x*-axis to provide for better visibility.) The onset of recrystallization is quite sharp, which implies possible suppression or even absence of the nucleation phase in the recrystallization process. Generally, the course of recrystallization isotherms is much less dependent on T_c than that of additional crystallization (Fig. 6) and, of course, of primary melt crystallization (Fig. 2). The Avrami plots of recrystallization shown in Figure 11 provided values of the kinetic parameters n and k [Fig. 12(a) and (b)].

The values of the recrystallization Avrami exponent n fall into a narrow range around 1.5 without any apparent dependency on T_c. From the average value of $n = 1.5$ we can speculate about two possible kinetic mechanisms of recrystallization. The first one would include partial melting of the primary crystallites ($T_m \approx 51$°C) followed by one-dimensional rearrangement of chains facilitated by the cooperative *gauche–trans* transition and resulting in increased perfection of lamellae. In the second mechanism, the primary crystallites would partially melt and, after the cooperative transition at 54°C leading to formation of the all-*trans* CH_2 sequences, the chain would rearrange by a two-dimensional mechanism, with the nucleation phase essentially missing, similarly to additional crystallization (see also Tan et al.[24]). Considering the shape of the recrystallization exotherms in Figure 9 and a sharp onset of the recrystallization isotherms in Figure 10, we suggest that the latter kinetic mechanism of recrystallization is more probable. However, the DSC method alone is obviously not able to definitely confirm the mechanism of additional crystallization and recrystallization of MPA.

The values of the kinetic constant k [Fig. 12(b)] imply that recrystallization at 54°C, as the third stage of the complex crystallization process of MPA, shows a very weak decreasing dependency of its rate on the original melt crystallization temperature T_c. As could be expected, the rate of recrystallization decreases with molecular weight of MPA. A comparison of the values of k of the three studied steps shows that recrystallization, similarly to additional crystallization, is a faster process, by several orders of magnitude, than melt crystallization. Apparently, the absence of the kinetic nucleation phase is in play here.

Comparison of experimental and calculated cumulative recrystallization isotherms is presented in Figure 10. One can see that, in this case, the Avrami approach holds true up to degrees of recrystallization

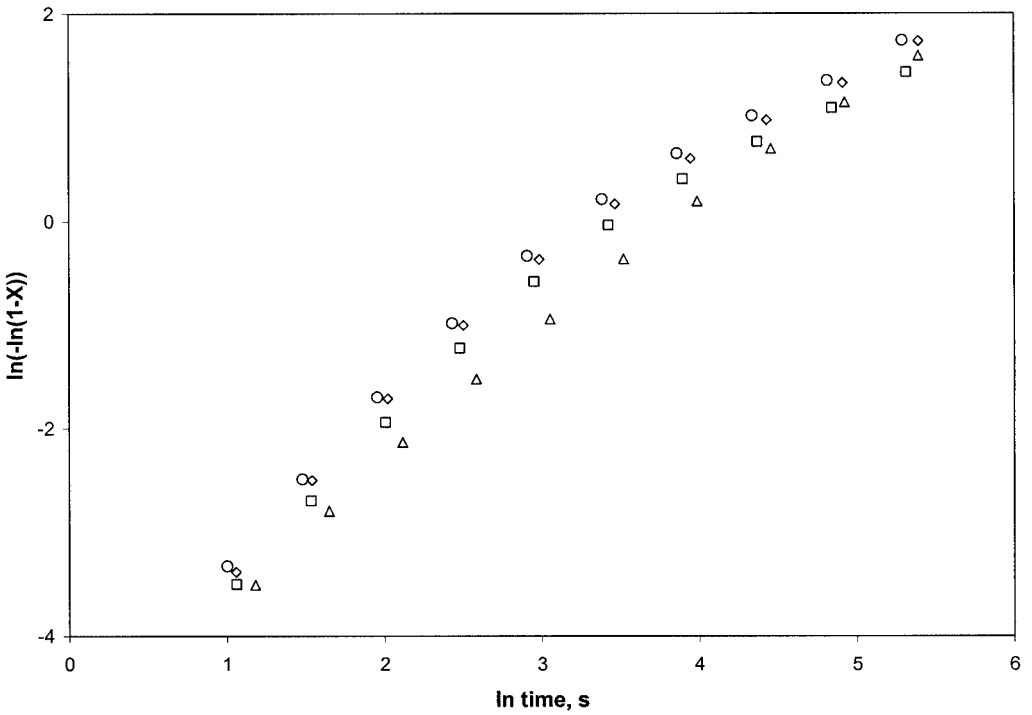

Figure 11 Avrami plots of recrystallization of MPA 5 at 54°C after melt crystallization at respective T_c and additional crystallization at 30°C; ○ −10°C; ◇ 0°C; △ 10°C; □ 20°C.

30–40% for T_c values of −10, 0, and 20°C. Its validity, however, is limited to about 15% for T_c = 10°C.

Activation energy

The three steps of the complex crystallization/recrystallization behavior of MPA were assumed to be thermally activated. A generally applied tool in evaluating activation energy of isothermal kinetic processes is the Arrhenius equation[25]:

$$K = k_0 \exp(-\Delta E/RT_c) \qquad (2)$$

where K is the crystallization rate, k_0 is a temperature-independent preexponential factor, and R is the universal gas constant. Thus, activation energy ΔE is usually obtained from a plot of ln K against $1/T$. In our case, K was expressed as a slope of the tangent to the experimental cumulative isotherms in their inflection point (Figs. 2, 6, and 10). This approach, unlike the method using the crystallization rate parameter $k^{1/n}$ calculated from Avrami parameters, has an advantage of being independent of any particular kinetic model. The Arrhenius plots for the three steps of MPA 5 crystallization are shown in Figure 13. The activation energies obtained for primary melt crystallization, additional crystallization, and recrystallization of MPA from these plots are summarized in Table I.

The total activation energy ΔE consists of the free energy of formation of nuclei of critical size at respective T_c and the activation energy required for transporting molecular segments across the phase boundary to the crystallization surface. According to this definition, total activation energy ΔE is relevant only for the primary melt crystallization for which the values of ΔE about −55 kJ/mol were found. In the case of additional crystallization and recrystallization, ΔE represents the above-mentioned transport activation energy. It is virtually a measure of the dependency of rates of these processes on the original melt crystallization temperature T_c and, thus, it reflects some kind of memory of the system.

The negative signs of the values of ΔE for the three steps shown in Table I mean that the system should release energy when transforming from the molten to crystalline state and then to the higher-crystalline structure.

As shown above [Fig. 8(b)], two markedly different regions were found in the dependency of the additional crystallization rate on T_c. This is also apparent from the broken Arrhenius plot for additional crystallization in Figure 13 (dashed part of the plot suggests that drawing of lines in this region is speculative only). In the range of T_c values of −10 to 4.9°C (LT in Table I), the rate constant is almost independent of T_c and the corresponding values of ΔE are quite low. On the other hand, in the range of T_c values from 4.9 to 20°C (HT in Table I), the additional crystallization rate is strongly dependent on the original melt crystalliza-

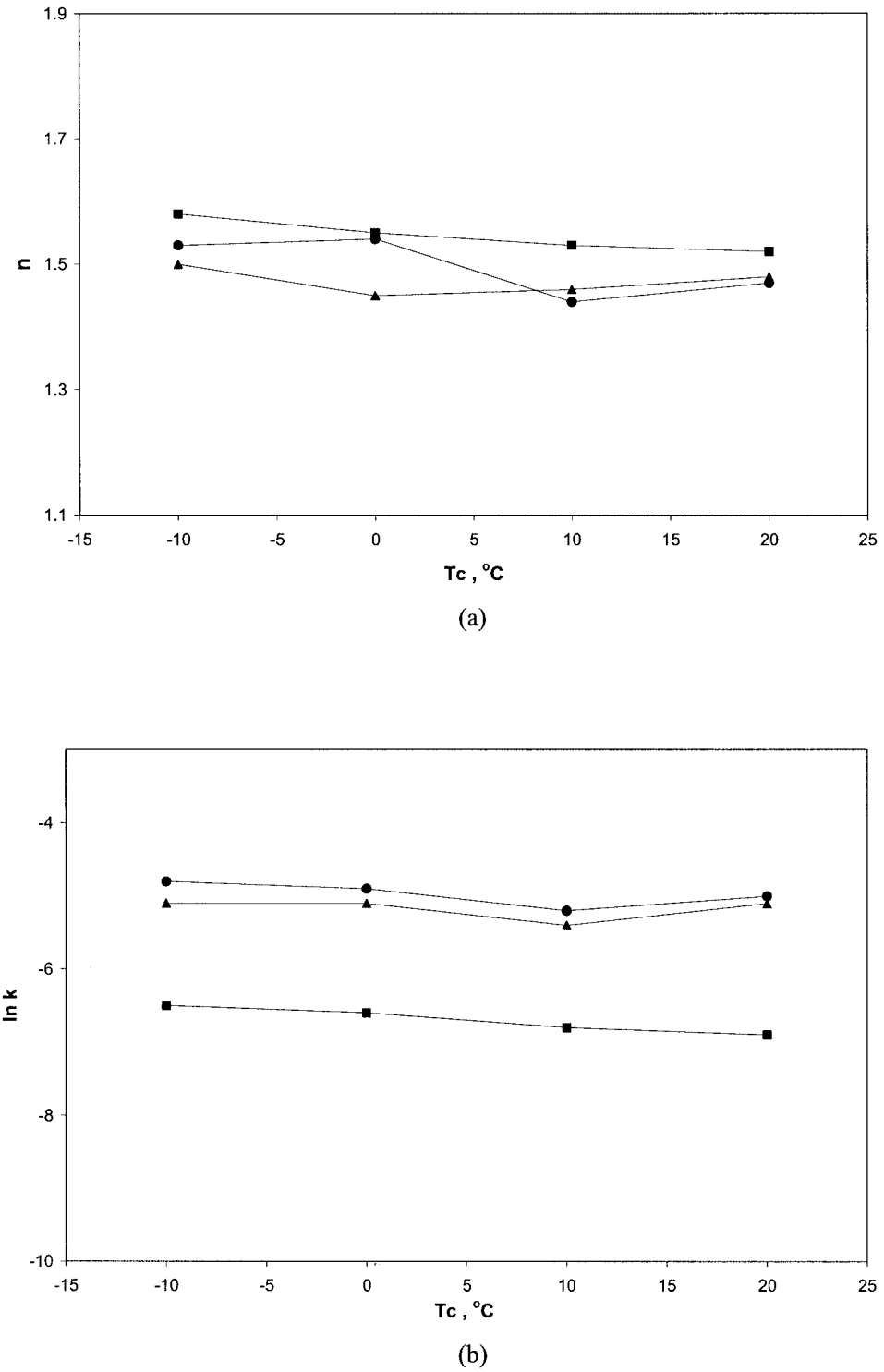

Figure 12 Dependency of kinetic parameters of recrystallization on melt crystallization temperature T_c: (a) Avrami exponent, (b) logarithm of rate constant; ● MPA 5; ▲ MPA 15; ■ MPA 45.

tion temperature and, consequently, the corresponding values of ΔE are relatively high.

The rate of recrystallization shows a very weak dependency on the original T_c [see Fig. 12(b)] and, consequently, the corresponding values of activation energy ΔE are quite low.

CONCLUSIONS

The Avrami theory was adopted in investigating the kinetics of the three isothermal steps involved in the complex crystallization process of poly(*N*-methyldodecano-12-lactam) (MPA), as studied by the DSC method:

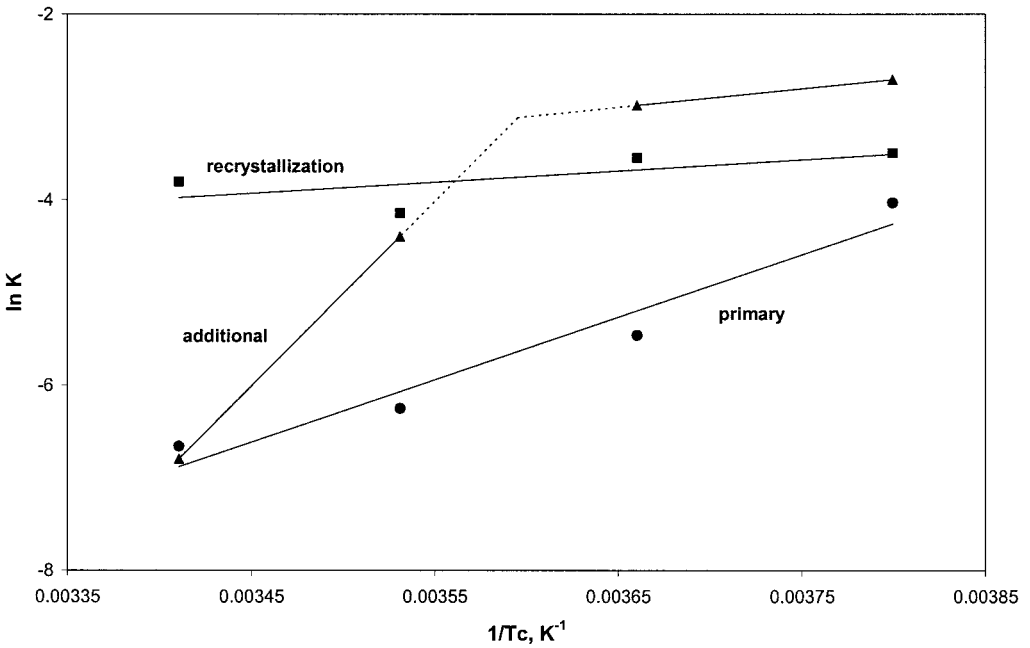

Figure 13 Dependency of rate constants of MPA 5 on reciprocal primary crystallization temperature T_c: ● primary crystallization; ▲ additional crystallization; ■ recrystallization.

1. Primary crystallization from the melt at a given temperature for T_c values ranging from −10 to 20°C
2. Additional crystallization at the optimum temperature of 30°C
3. Recrystallization at the optimum temperature of 54°C

The Avrami exponent of primary melt crystallization decreases between 2.5 and 1.9 with increasing T_c. This suggests heterogeneous athermal nucleation followed by two-dimensional lamellar crystal growth. At greater supercoolings, the homogeneous thermal nucleation is apparently involved to a greater extent. The kinetic constant decreases with T_c, in compliance with the nucleation-controlled mode of melt crystallization. MPA shows a high crystallization rate at temperatures quite close to T_g. This could be explained by the combination of a relatively high mobility of MPA chains, facilitated by their molecular structure, and a strong involvement of thermodynamic fluctuations, leading to homogeneous nucleation at temperatures close to T_g. Comparison of experimental and calculated cumulative isotherms has shown that the Avrami approach holds true up to relative crystallinities of 60 and 30% for T_c values of −10 and 0°C, respectively. For T_c values of 10 and 20°C, the upper limit of applicability is 10–15%.

Additional crystallization reached its maximum rate almost immediately after the temperature of the system was increased to 30°C. The Avrami exponent shows the value of about 1.5 independently of the original T_c. This implies a two-dimensional diffusion-controlled crystal growth with the missing nucleation phase. Thus, the primary melt crystallization process simply continues in the additional crystallization step, during which the volume of primary lamellae increases. The rate of additional crystallization is higher, by several orders of magnitude, than that of primary melt crystallization. In the range of T_c values of −10 to

TABLE I
Activation Energies of MPA Crystallization Steps (kJ mol^{-1})

Material	Primary	Additional		Recrystallization
		LT[a]	HT[b]	
MPA 5	−56.1	−16.6	−165.9	−9.9
MPA 15	−54.7	−17.1	−119.7	−6.5
MPA 45	−57.8	−25.6	−151.2	−9.8

[a] Range of T_c: −10 to 4.9°C.
[b] Range of T_c: 4.9 to 20°C.

0°C, the rate is almost independent of the original melt crystallization temperature. In the range of T_c values of 0 to 20°C, it sharply decreases with T_c. The Avrami approach holds true up to a crystallinity of 60% for additional crystallization after T_c values of −10 and 0°C. For higher T_c the upper limit of applicability is 10–20%.

The onset of recrystallization at 54°C is quite sharp, which implies the absence of the nucleation phase in the recrystallization process. The Avrami exponent shows the value of about 1.5 independently of T_c. The possible mechanism of recrystallization includes partial melting of crystallites formed during the melt and additional crystallization stages, cooperative transition to all-*trans* CH_2 sequences, and two-dimensional rearrangement of chains into the final, more perfect structure. Recrystallization at 54°C, as the third stage of the complex crystallization process of MPA, shows a very weak decreasing dependency of its rate on the original melt crystallization temperature T_c. The rate of recrystallization, similarly to additional crystallization, is by several orders of magnitude higher than that of melt crystallization. In the case of MPA recrystallization, applicability of the Avrami theory is limited by degrees of recrystallization of 30 to 40%.

The values of activation energy ΔE for the three stages of MPA crystallization were derived from the Arrhenius equation, wherein rates of the respective crystallization steps were expressed as slopes of tangents to the cumulative crystallization isotherms in their inflection points. The negative sign of ΔE for all three steps means that the system should release energy when transforming from the molten to crystalline state and then to a higher-crystalline structure. ΔE of primary melt crystallization is approximately −55 kJ/mol. Additional crystallization shows a broken Arrhenius plot, leading to quite low values (∼ −20 kJ/mol) of ΔE for lower T_c, and relatively high values (∼ −145 kJ/mol, on average) for higher T_c. Recrystallization of MPA shows a very weak dependency of its rate on the original T_c and, consequently, low values (∼ −9 kJ/mol) were found for the activation energy of this process.

The authors thank the Grant Agency of the Academy of Sciences of the Czech Republic (Grant A4050007) for financial support.

References

1. Kratochvíl, J.; Sikora, A.; Baldrian, J.; Dybal, J.; Puffr, R. Polymer 2000, 41, 7653.
2. Kratochvíl, J.; Sikora, A.; Baldrian, J.; Dybal, J.; Puffr, R. Polymer 2000, 41, 7667.
3. (a) Avrami, M. J. Chem Phys 1939, 7, 1103; (b) Avrami, M. J. Chem Phys 1940, 8, 212.
4. Mandelkern, L.; Quinn, F. A.; Flory, P. J. J Appl Phys 1954, 25, 830.
5. Hinrichs, V.; Kalinka, G.; Hinrichsen, G. J. Macromol Sci Phys B 1996, 35, 295.
6. Srinivas, S.; Babu, J. R.; Riffle, J. S.; Wilkes, G. L. Polym Eng Sci 1997, 37, 497.
7. Verhoyen, O.; Dupret, F.; Legras, R. Polym Eng Sci 1998, 38, 1594.
8. Muellerleile, J. T.; Risch, B. G.; Rodrigues, D. E.; Wilkes, G. L.; Jones, D. M. Polymer 1993, 34, 789.
9. Woo, E. M.; Chen, J. M. J Polym Sci Part B: Polym Phys 1995, 33, 1985.
10. Zhong, Z.; Guo, Q. Polymer 2000, 41, 1711.
11. Lopez-Manchado, M. A.; Arroyo, M. Polymer 1999, 40, 487.
12. Lu, X.; Hay, J. N. Polymer 2000, 41, 7427.
13. Cho, K.; Li, F.; Choi, J. Polymer 1999, 40, 1719.
14. Long, Y.; Shanks, R. A.; Stachurski, Z. H. Prog Polym Sci 1995, 20, 651.
15. Ratta, V.; Ayambem, A.; Young, R.; McGrath, J. E.; Wilkes, G. L. Polymer 2000, 41, 8121.
16. Seo, Y.; Kim, J.; Kim, K. U.; Kim, Y. C. Polymer 2000, 41, 2639.
17. Li, B.; Yu, J.; Lee, S.; Ree, M. Polymer 1999, 40, 5371.
18. Liu, S.; Yu, Y.; Cui, Y.; Zhang, H.; Mo, Z. J Appl Polym Sci 1998, 70, 2371.
19. Naga, N.; Mizunuma, K.; Sadatoshi, H.; Kakugo, M. Polymer 2000, 41, 203.
20. Chisholm, B. J.; Zimmer, J. G. J Appl Polym Sci 2000, 76, 1296.
21. Mandelkern, L. Crystallization of Polymers; McGraw-Hill: New York, 1964.
22. Kratochvíl, J.; Sikora, A. J Appl Polym Sci, to appear.
23. Wang, J.; Cao, J.; Chen, Y.; Ke, Y.; Wu, Z.; Mo, Z. J Appl Polym Sci 1996, 61, 1999.
24. Tan, S.; Su, A.; Li, W.; Zhou, E. J Polym Sci Part B: Polym Phys 2000, 38, 53.
25. Cebe, P.; Hong, S. D. Polymer 1986, 27, 1183.